IEEE Photonics Journal
An IEEE Photonics Society Publication

Open Access

Silicon Nitride/Silicon Dioxide Echelle Grating Spectrometer for Operation Near 1.55 μm

Volume 10, Number 6, December 2018

Shengjie Xie
Yang Meng
Joss Bland-Hawthorn
Sylvain Veilleux
Mario Dagenais, *Fellow, IEEE*

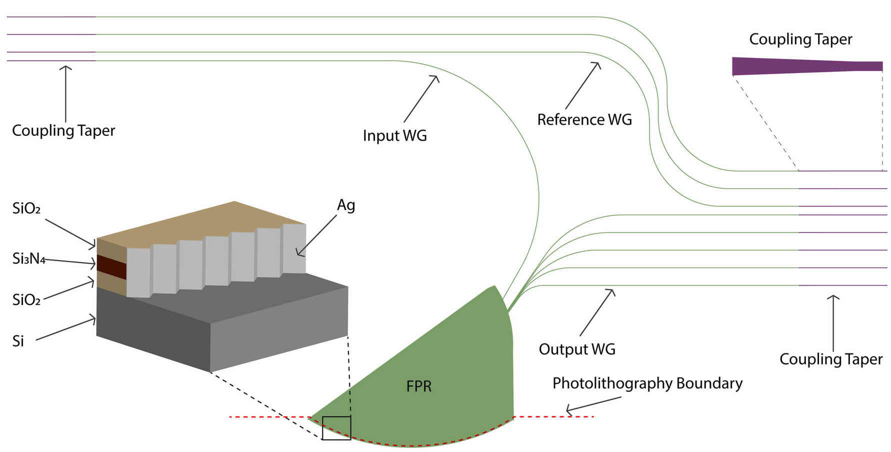

DOI: 10.1109/JPHOT.2018.2880182

Silicon Nitride/Silicon Dioxide Echelle Grating Spectrometer for Operation Near 1.55 μm

Shengjie Xie,[1] Yang Meng,[1] Joss Bland-Hawthorn,[2] Sylvain Veilleux,[3] and Mario Dagenais,[1] *Fellow, IEEE*

[1]Department of Electrical and Computer Engineering, University of Maryland, College Park, MD 20742 USA
[2]Sydney Institute for Astronomy and Sydney Astrophotonic Instrumentation Labs, School of Physics, University of Sydney, Sydney NSW 2006, Australia
[3]Department of Astronomy and Joint Space-Science Institute, University of Maryland, College Park, MD 20742 USA

DOI:10.1109/JPHOT.2018.2880182

Manuscript received August 30, 2018; revised October 19, 2018; accepted October 23, 2018. Date of publication November 16, 2018; date of current version November 22, 2018. This work was supported in part by the W. M. Keck Foundation grant, in part by the National Science Foundation under Grant ATI 1711377, and in part by the NASA under Grant 16-APRA16-0064. *(Shengjie Xie and Yang Meng contributed equally to this work.)* Corresponding author: Mario Dagenais (e-mail: dage@ece.umd.edu).

Abstract: Here we use an electron beam lithography system to pattern an Si_3N_4/SiO_2 echelle grating using silver as a reflector on the grating grooves. The grating in this letter achieves 1.39 dB on-chip loss, a spectral resolution of $\sim$1300, a 1.2 dB channel nonuniformity, and less than -30 dB adjacent channel crosstalk for the transverse electric field polarization. We establish that stitching errors can lead to appreciable adjacent channel crosstalk if proper precaution is not taken to minimize them.

Index Terms: nanophotonics, spectroscopy, demultiplexing

1. Introduction

It is expected that an on-chip spectrometer will become an important building block for wavelength-division-multiplexed nanophotonics applications. Among many types of on-chip spectrometers, echelle gratings and arrayed waveguide gratings (AWG) are two major candidates. The echelle grating can be designed to have a smaller footprint when compared with an AWG of similar performance, which makes it easier to integrate echelles with other photonic integrated devices [1]. Furthermore, its small footprint can also minimize the phase error generated due to modal index variation in the light transmission, which is an important source of crosstalk and losses. Hence echelle has attracted increasing interest in recent years. Different material systems have been reported as potential platforms for implementing echelle grating, including silicon-on-insulator (SOI) [2]–[7], silicon nitride (Si_3N_4/SiO_2) [8], silica on silicon [9], silicon-germanium [10], InP [11] etc. While most research centers on SOI, which benefits from its high index contrast and its CMOS compatibility, Si_3N_4/SiO_2 has also unique advantages since it is transparent in both near infrared and the visible spectral regions. Si_3N_4/SiO_2 can be a perfect platform for applications requiring transparency between 1.0–1.7 μm such as for astrophotonics [12]–[15]. In addition to the broadband working wavelength, the moderate index contrast of Si_3N_4/SiO_2 will provide insensitivity to sidewall roughness and phase errors, both of which are critical for a low loss, high performance on-chip spectrometer. This is of great importance for many photonic applications such as for astrophotonics spectrometers and filtering applications for quantum information [16].

For an echelle, light incident from the input waveguide propagates through a free propagation region (FPR), is reflected by silver deposited on the grating sidewall, and is refocused on the output waveguide. Since there are constant phase differences between different paths, constructive interference occurs on each output waveguide at different wavelength and hence the incident light is spectrally resolved. Previously, most researchers have used a distributed Bragg grating (DBG) as the reflector because it can achieve high reflectivity within the designed stop band and it is easy to fabricate – the DBG reflector and the remaining part of the echelle grating can be defined at the same time [2]–[5]. However, according to the Bragg grating theory, the photonic stopband bandwidth is given by $\Delta\lambda_{gap} = 2|\frac{n_1}{n_0}|\lambda_0$, where n_0 is the average refractive index, n_1 is the amplitude of the index modulation, and is roughly evaluated to be around 200 nm. Thus, a DBG is not considered an ultra-broad band reflector if spectroscopy over a wide spectral range is required. Silver is a perfect candidate because of its ultra-high reflectivity (more than 98%) over an ultra-wide bandwidth (from 400 nm to more than 20 μm) [17] and because of its simplicity.

In this paper, we demonstrate 5 channels, EBL written, Si_3N_4/SiO_2 echelle grating centered at 1550 nm with 5 nm channel spacing. The echelle grating features a 1.39 dB insertion loss, a spectral resolution ($\lambda/\Delta\lambda$) of $\sim$1300, a 1.2 dB channel non-uniformity, and less than -30 dB adjacent channel crosstalk for the transverse electric (TE) field polarization. The combined performance of the echelle grating is better than for any other echelle gratings reported in the literature. Using a deposited silver thin film as a light reflector, the echelle grating demonstrated in this paper has potential for ultra-broadband spectroscopy. We also analyze and experimentally demonstrate that stitching errors can be the major source of adjacent channel crosstalk for e-beam written echelle gratings.

2. Design and Fabrication

To start the design, we first chose the Si_3N_4 layer thickness to be 300 nm. There are several reasons for choosing this thickness. When silver is used as a reflector, the metal needs to be coated on the facet of the etched grating grooves to cover the whole optical mode in the vertical direction and achieve ultra-high reflectivity ($\sim$98–99% at 1550 nm). Thinner Si_3N_4 leads to larger optical mode that requires deeper etching for that light reflection. Very deep etching is difficult to achieve and may potentially create large sidewall roughness and non-vertical facets, which will result in large optical losses. Although thicker Si_3N_4 can achieve a more confined slab waveguide optical mode, it is more difficult to control the film stress in a thick Si_3N_4 film contained between two SiO_2 layers. Therefore, the vertical mode should be moderately confined. A 300 nm Si_3N_4/SiO_2 slab waveguide has a calculated 0.73 μm vertical mode size for the TE mode at 1550 nm and is chosen in this work. Fig. 1 shows the schematic layout of the simulated echelle grating. We have designed the echelle grating spectrometer using a Rowland circle configuration [18]. Here, we have used waveguides (WGs) with an area given by 900×300 nm that includes the input, output and reference WGs. The Rowland circle radius is 700 μm and the grating length is 1400 μm. High efficiency coupling tapers are used at the input and output facets of the sample as mode converters to minimize the fiber-waveguide coupling loss [19]. We use the 10th diffraction order to define the input and output waveguide positions. We have simulated 5 channels spaced by 5 nm centered at 1550 nm and optimized for TE mode.

As shown in Fig. 2, The fabrication starts with a silicon wafer with a 10 μm thermally grown oxide (SiO_2) layer on top. Then, 300 nm low-pressure chemical vapor deposition (LPCVD) Si_3N_4 is deposited and 1.3 μm plasma-enhanced chemical vapor deposition (PECVD) SiO_2 is finally deposited. We then spin coat ZEP-520A, a positive tone e-beam resist. Then the echelle grating is patterned with 100 kV EBL system. An 80 nm chromium hard mask is deposited by e-beam deposition as the etching hard mask. After that, fluorine gas based inductively coupled plasma (ICP) etching is used to form WGs and deep, vertical grating facet. As mentioned before, silver should

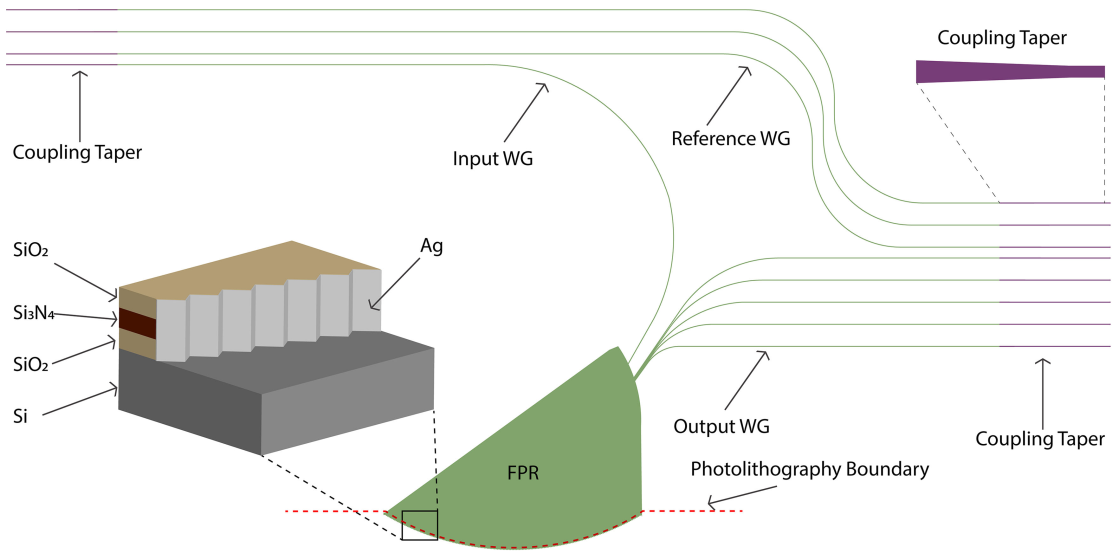

Fig. 1. Schematic layout of the echelle grating. The light incidents from the input waveguide, propagates through the FPR, is reflected by the grating and is refocused on the output WGs. 3 Reference WGs are used to subtract the propagation loss and coupling loss. The dashed red line shows the photolithography boundary. The inset shows the schematic tilted view of the grating teeth. Deep etch is used for silver deposition.

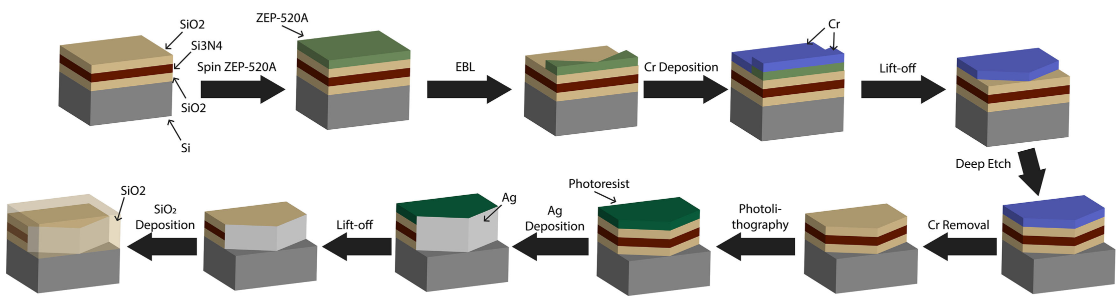

Fig. 2. Fabrication process of the proposed echelle grating.

cover the vertical mode at the grating teeth to get perfect reflectivity. Here, we have etched 1.3 μm PECVD SiO_2, 300 nm LPCVD Si_3N_4, and 1.5 μm thermal SiO_2. Then another photolithography step is used to define the boundary for silver deposition. As shown in Figs. 1 and 2, after the photolithography process, all patterns above the photolithography boundary are protected by the photoresist, silver will only be deposited on the surface below the photolithography boundary so that only the grating facets are covered by silver while the FPR and WGs are free from silver deposition. To make sure the silver is deposited on the grating sidewall, the sample is tilted 90 degrees during silver deposition so that the sidewall is facing toward the silver source. 130 nm silver is deposited with e-beam deposition. Finally, 6 μm of PECVD SiO_2 is deposited as a top cladding layer. As shown in Fig. 3, EBL ensures that a precise and smooth grating is created with good waveguide definition. In Fig. 3(c), we can see that the ICP etching process achieved vertical and deep etch, both of which are critical for low loss echelle grating.

3. Experimental Result

To characterize the transmission spectrum of the echelle grating, a TE polarized tunable laser is used as the light source. The light travels through a polarization-maintaining (PM) fiber and is

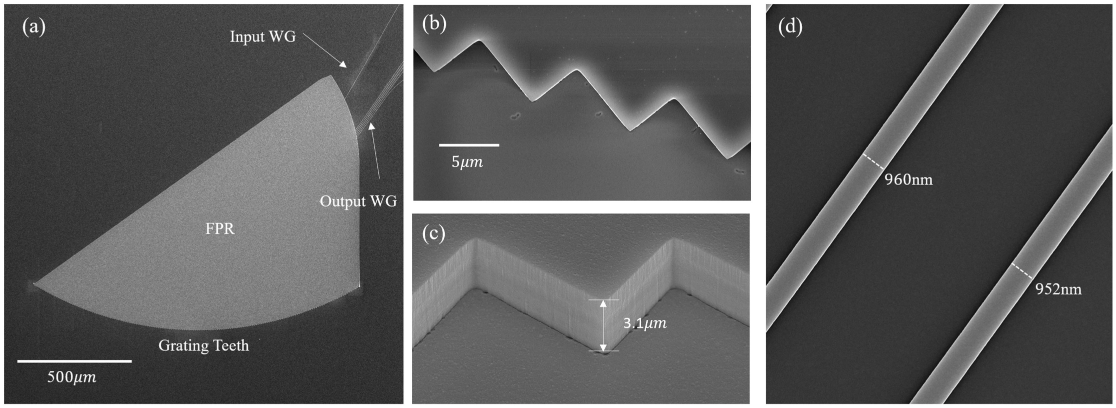

Fig. 3. SEM image of the echelle grating. (a) Top view of the echelle grating showing the relative position of WGs and grating teeth. (b) Zoom in image of the grating teeth before deep etching. Grating teeth get precise definition with EBL. (c) The etched facets of the echelle grating covered with silver. 3.1 μm deep etch was achieved by ICP etching with perfect verticality. (d) Zoom in image of the output WGs with smooth edge.

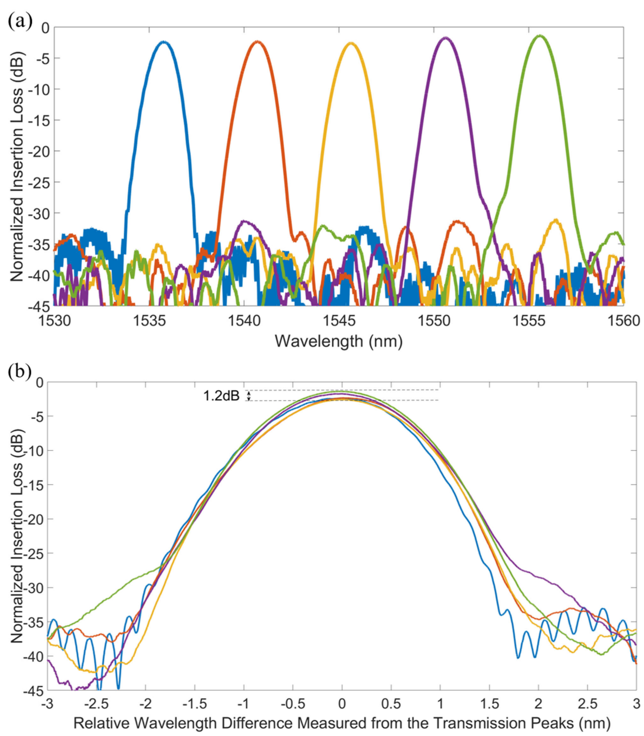

Fig. 4. (a) Measured TE mode transmission pattern of the echelle grating. (b) Superimposed transmission pattern of the fabricated echelle grating's five channels. Very good overlap and a maximum transmission power non-uniformity of 1.2 dB are achieved in our echelle grating.

coupled into the chip with an appropriate rectangular waveguide followed with an inverse taper. A fiber rotator is used to ensure that the input light is TE polarized. The output WGs are coupled out using a PM fiber and the signal is measured by a power meter.

Fig. 4(a) shows the TE transmission pattern of the echelle grating. The insertion loss is normalized to the reference waveguide to subtract the linear propagation loss and fiber-waveguide coupling loss. The echelle grating is centered at 1545.622 nm with a 4.929 ± 0.075 nm channel spacing. The

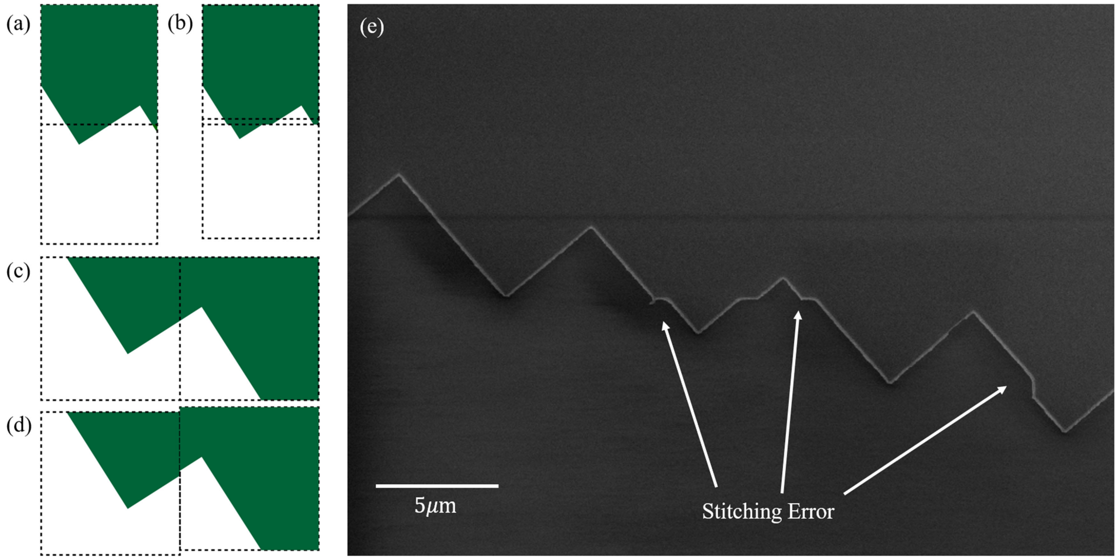

Fig. 5. Schematic layout and SEM image of stitching error. (a–d) Schematic layouts of stitch-free e-beam patterning and e-beam patterning with stitching error. These errors can happen at both left-right boundaries and up-down boundaries (e) SEM image of stitching errors on grating grooves.

best insertion loss of the echelle grating is 1.39 dB. The FWHM of each channel is 1.207 nm and hence the spectral resolution ($\lambda/\Delta\lambda$) is about 1300. The adjacent channel crosstalk is more than 30 dB down for all 5 channels. Comparing with the simulation result, the channel center wavelength is shifted by 4.578 nm from the designed center wavelength. This is mainly attributed to the refractive index uncertainty of Si_3N_4/SiO_2 and to phase error generated in the FPR propagation. Fig. 4(b) shows that the channel non-uniformity is 1.2 dB. All of this indicates that Si_3N_4/SiO_2 echelle grating with a silver reflector is a good platform for implementing future broadband on-chip spectrometer and deserves proper consideration.

Crosstalk is always a concern in spectroscopy. Typically, the main source of the crosstalk is phase error generated from the non-uniformity of FPR. However, we discovered that for an EBL fabricated echelle grating, the stitching error can be a dominant source of crosstalk [20]. As shown in Fig. 5, the e-beam system works in the following way: the software divides the whole pattern into several grids, which are called writing fields (WFs). The electron beam gun will sit on a single WF, write all patterns inside the WF, and then move to the next WF until all WFs are written. The stitching error comes from the imperfect WF alignment and imprecise stage moving. This can happen in a periodic manner. For general e-beam fabricated structures, such stitching errors may just add extra losses. Such periodic stitching error, however, will work like another grating structure overlapping with the original design and thus will deteriorate the performance of echelle grating.

We have used 100 μm and 200 μm WF size in our experiment. As shown in Fig. 6(a) and (c), by adding periodic offset on the grating grooves, the simulation shows that, when 100 μm periodic stitching error exists on the grating, there are several satellite peaks in each channel with 10 nm spacing, while for 200 μm the satellite peaks spacing decrease to 5 nm. This is because, in the original design, we were using the 10th order for our echelle. If we view the periodic stitching error as a grating that has the same Rowland circle geometry but now 100 μm or 200 μm grating period, then the 125th, or 250th, order of light is focused in the center of the output channels. The corresponding free spectral ranges (FSRs) are 10 nm and 5 nm. Such small FSRs are undesirable for the echelle grating because it overlaps with the normal signals and increases the crosstalk level dramatically. Experimentally, we observed the small FSR indicated in the simulation. The crosstalk level increased from less than -30 dB to about -10 dB as shown in Fig. 6(b) and (d). The insertion

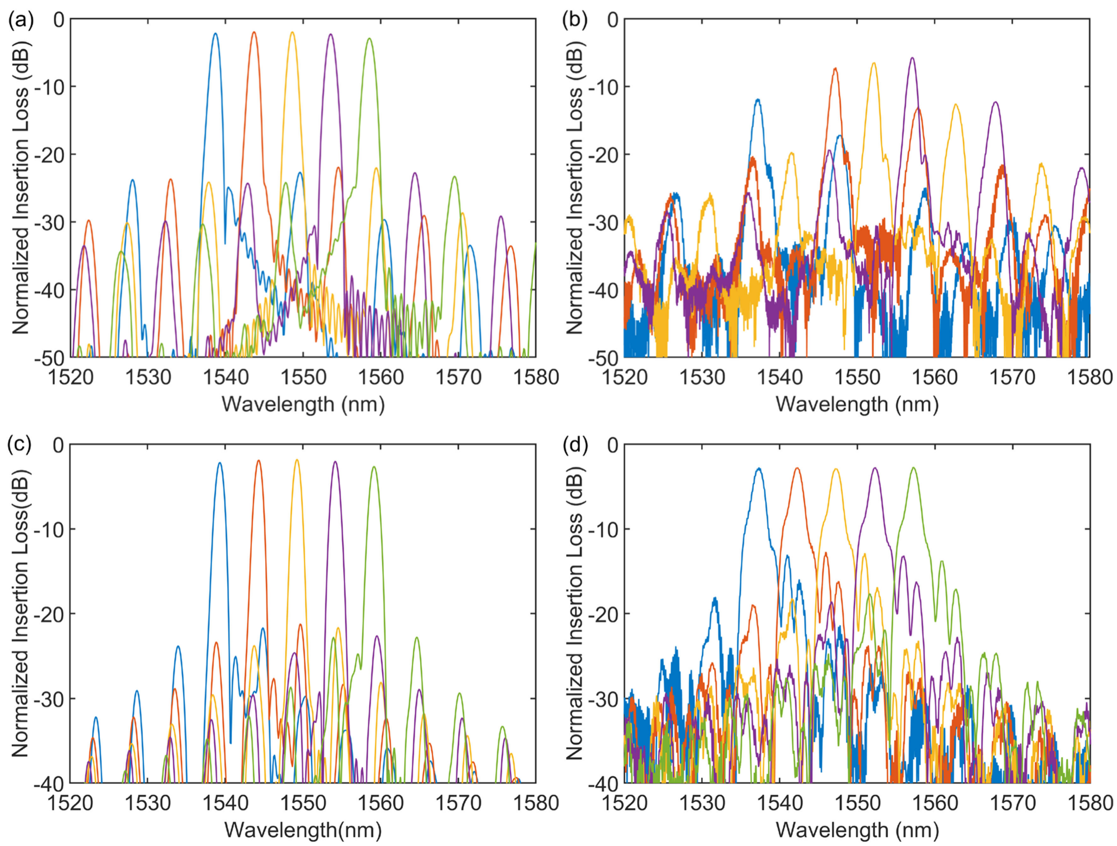

Fig. 6. Influence of stitching errors on adjacent channel crosstalk. (a) Simulation results of 100 μm WF transmission pattern with stitching errors. (b) Experimental results of 100 μm WF transmission pattern with stitching errors. (c) Simulation results of 200 μm WF transmission pattern with stitching errors. (d) Experimental results of 200 μm WF transmission pattern with stitching errors.

loss also increased from 1.39 dB to more than 5 dB and 2.8 dB, when the echelle grating suffers from periodic 100 μm and 200 μm stitching error, respectively. Compared with phase errors in the FPR, the stitching errors can be a dominant factor for crosstalk in EBL fabricated echelle grating. Potential solutions to the stitching error problem include: better field alignment; spin coating a conducting layer (i.e., Aquasave) on top of the e-beam resist to get rid of charging effects; use of a larger writing field so that the grating grooves will be patterned in one single writing field; use a more stable e-beam system or an advanced photolithography system so that no writing field is involved in the exposure process.

4. Conclusion

In this paper, we have demonstrated the design, fabrication and characterization of a 5-channel Si_3N_4/SiO_2 echelle grating with silver as a reflector. The grating experimentally achieved 1.39 dB insertion loss, 4.929 nm channel spacing, a 1300 spectral resolution, a 1.2 dB channel non-uniformity and better than -30 dB crosstalk. This performance is better than for any other echelle grating reported in literature. We also report that stitching errors that can arise in e-beam written patterns can be a dominant crosstalk mechanism for photonic gratings unless stitching errors are minimized. In our measurements, we have demonstrated that good performance can be obtained for e-beam written echelle gratings. This should lead to new applications in future where on-chip broadband and low loss spectrometers is are desired.

Acknowledgement

The authors would like to thank the staff at the University of Maryland Nanocenter fabrication laboratory for their help with the various fabrication techniques. They also thank Y. Hu and S. Dutt for providing useful suggestions.

A. W. M. Keck Foundation grant, a National Science Foundation grant (ATI 1711377) and a NASA grant (16-APRA 16-0064) are duly acknowledged.

References

[1] S. Pathak, P. Dumon, D. V. Thourhout, and W. Bogaerts, "Comparison of AWGs and echelle gratings for wavelength division multiplexing on silicon-on-insulator," *IEEE Photon. J.*, vol. 6, no. 5, Oct. 2014, Art. no. 4900109.

[2] X. Pommarede *et al.*, "16 $\times$ 100 GHz echelle grating-based wavelength multiplexer on silicon-on-insulator platform," *IEEE Photon. Technol. Lett.*, vol. 29, no. 6, pp. 493–495, Mar. 2017.

[3] C. Sciancalepore *et al.*, "Low-crosstalk fabrication-insensitive echelle grating demultiplexers on silicon-on-insulator," *IEEE Photon. Technol. Lett.*, vol. 27, no. 5, pp. 494–497, Mar. 2015.

[4] M. Muneeb *et al.*, "Demonstration of Silicon-on-insulator mid-infrared spectrometers operating at 3.8 μm," *Opt. Exp.*, vol. 21, no. 10, pp. 11659–11669, 2013.

[5] W. Bogaerts *et al.*, "Silicon-on-insulator spectral filters fabricated with CMOS technology," *IEEE J. Sel. Topics Quantum Electron.*, vol. 16, no. 1, pp. 33–44, Jan./Feb. 2010.

[6] D. Feng *et al.*, "Fabrication insensitive echelle grating in silicon-on-insulator platform," *IEEE Photon. Technol. Lett.*, vol. 23, no. 5, pp. 284–286, Mar. 2011.

[7] X. Ma, M. Li, and J. He, "CMOS-compatible integrated spectrometer based on echelle diffraction grating and MSM photodetector array," *IEEE Photon. J.*, vol. 5. no. 2, Apr. 2013, Art. no. 6600807.

[8] E. Ryckeboer *et al.*, "CMOS-compatible silicon nitride spectrometers for lab-on-a-chip spectral sensing," *Proc. SPIE*, vol. 9891, 2016, Art. no. 98911K.

[9] S. Janz *et al.*, "Planar waveguide echelle gratings in silica-on-silicon," *IEEE Photon. Technol. Lett.*, vol. 16, no. 2, pp. 503–505, Feb. 2004.

[10] A. Malik, M. Muneeb, Y. Shimura, J. V. Campenhout, R. Loo, and G. Roelkens, "Germanium-on-silicon planar concave grating wavelength (de) multiplexers in the mid-infrared," *Appl. Phys. Lett.*, vol. 103, 2013, Art. no. 161119.

[11] J. Pello, M. Muneeb, S. Keyvaninia, J. J. G. M. van der Tol, G. Roelkens, and M. K. Smit, "Planar concave grating demultiplexers on an InP-membrane-on-silicon photonic platform," *IEEE Photon. Technol. Lett.*, vol. 25, no. 20, pp. 1969–1972, Oct. 2013.

[12] J. Bland-Hawthorn and A. Horton, "Instruments without optics: An integrated photonic spectrograph," *Proc. SPIE*, vol. 6269, 2006, Art. no. 62690N.

[13] J. Bland-Hawthorn *et al.*, "PIMMS: Photonic integrated multimode microspetrograph," *Proc. SPIE*, vol. 7735, 2010, Art. no. 77350N.

[14] P. Gatkine, S. Veilleux, Y. Hu, J. Bland-Hawthorn, and M. Dagenais, "Arrayed waveguide grating spectrometers for astronomical applications: New results," *Opt. Exp.*, vol. 25, no. 15, pp. 17918–17935, 2017.

[15] T. Zhu, Y. Hu, P. Gatkine, S. Veilleux, J. Bland-Hawthorn, and M. Dagenais, "Arbitrary on-chip optical filter using complex waveguide Bragg gratings," *Appl. Phys. Lett.*, vol. 108, 2016, Art. no. 101104.

[16] N. C. Harris *et al.*, "Integrated source of spectrally filtered correlated photons for large-scale quantum photonic systems," *Phys. Rev. X*, vol. 4, no. 4, pp. 1–10, 2014.

[17] H. U. Yang, J. D'Archangel, M. L. Sundheimer, E. Tucker, G. D. Boreman, and M. B. Raschke, "Optical dielectric function of silver," *Phys. Rev. B*, vol. 91, no. 23, 2015, Art. no. 235137.

[18] R. J. Meltzer, "Spectrographs and monochromators," *Appl. Opt. Opt. Eng.*, vol. 5, pp. 47–84, 1969.

[19] T. Zhu, Y. Hu, P. Gatkine, S. Veilleux, J. Bland-Hawthorn, and M. Dagenais, "Ultrabroadband high coupling efficiency fiber-to-waveguide coupler using Si_3N_4/SiO_2 waveguides on silicon," *IEEE Photon. J.*, vol. 8, no. 5, 2016, Art. no. 7102112.

[20] J. He, B. Lamontagne, A. Delâge, L. Erickson, M. Davies, and E. S. Koteles, "Monolithic integrated wavelength demultiplexer based on a waveguide Rowland circle grating in InGaAsP/InP," *J. Lightw. Technol.*, vol. 16, no. 4, pp. 631–638, Apr. 1998.